Handedness and its genetic influences are associated with structural asymmetries of the cerebral cortex in 31,864 individuals

Zhiqiang Sha[a], Antonietta Pepe[b,c,d], Dick Schijven[a], Amaia Carrión-Castillo[a,e], James M. Roe[f], René Westerhausen[g], Marc Joliot[b,c,d], Simon E. Fisher[a,h], Fabrice Crivello[b,c,d], and Clyde Francks[a,h,1]

[a]Language and Genetics Department, Max Planck Institute for Psycholinguistics 6525 XD Nijmegen, The Netherlands; [b]Groupe d'Imagerie Neurofonctionnelle, Université de Bordeaux, Bordeaux F-33000, France; [c]Groupe d'Imagerie Neurofonctionnelle, Commissariat à l'énergie atomique et aux énergies alternatives, Bordeaux F-33000, France; [d]Groupe d'Imagerie Neurofonctionnelle, Centre national de la recherche scientifique, Bordeaux F-33000, France; [e]Basque Center on Cognition, Brain and Language, San Sebastian 20009, Spain; [f]Center for Lifespan Changes in Brain and Cognition, Department of Psychology, University of Oslo, Oslo 0315, Norway; [g]Section for Cognitive and Clinical Neuroscience, Department of Psychology, University of Oslo, Oslo 0315, Norway; and [h]Donders Institute for Brain, Cognition and Behaviour, Radboud University, Nijmegen 6525 EN, The Netherlands

Edited by Michael C. Corballis, School of Psychology, University of Auckland, Auckland, New Zealand, and accepted by the Editorial Board October 12, 2021 (received for review July 16, 2021)

Roughly 10% of the human population is left-handed, and this rate is increased in some brain-related disorders. The neuroanatomical correlates of hand preference have remained equivocal. We resampled structural brain image data from 28,802 right-handers and 3,062 left-handers (UK Biobank population dataset) to a symmetrical surface template, and mapped asymmetries for each of 8,681 vertices across the cerebral cortex in each individual. Left-handers compared to right-handers showed average differences of surface area asymmetry within the fusiform cortex, the anterior insula, the anterior middle cingulate cortex, and the precentral cortex. Meta-analyzed functional imaging data implicated these regions in executive functions and language. Polygenic disposition to left-handedness was associated with two of these regional asymmetries, and 18 loci previously linked with left-handedness by genome-wide screening showed associations with one or more of these asymmetries. Implicated genes included six encoding microtubule-related proteins: *TUBB*, *TUBA1B*, *TUBB3*, *TUBB4A*, *MAP2*, and *NME7*—mutations in the latter can cause left to right reversal of the visceral organs. There were also two cortical regions where average thickness asymmetry was altered in left-handedness: on the postcentral gyrus and the inferior occipital cortex, functionally annotated with hand sensorimotor and visual roles. These cortical thickness asymmetries were not heritable. Heritable surface area asymmetries of language-related regions may link the etiologies of hand preference and language, whereas nonheritable asymmetries of sensorimotor cortex may manifest as consequences of hand preference.

brain asymmetry | left-handedness | cerebral cortex | gene–brain–behavior | polygenic scores

Roughly 90% of the human population is right-handed and 10% left-handed, and this strong bias is broadly consistent across cultures, ethnicities, and history (1–5). Hand motor control is performed primarily by the contralateral brain hemisphere, such that right-handedness reflects left-hemisphere dominance for hand articulation, and vice versa (6). Behavioral precursors of hand preference are established in the developing human fetus (7, 8), probably through a genetically regulated program of asymmetrical brain development (9–12). Left-handedness occurs at increased frequencies in neurodevelopmental and psychiatric conditions, including intellectual disability (13), autism (14), and schizophrenia (15). This suggests overlapping genetic and developmental contributions to altered brain asymmetry and psychiatric conditions. However, it is important to stress that the large majority of left-handed people do not have these conditions.

Despite decades of research, the brain anatomical correlates of hand preference have remained uncertain. Some MRI studies have reported slightly altered laterality of the sensorimotor cortex around the central sulcus as well as temporal auditory cortex in left-handed people—while other studies found no effects at all (16–22). Most of these studies focused on hypothesis-driven regions of interest rather than mapping across the entire cerebral cortex, and they used different methods of analysis and measurement. The results were conflicting, not replicated or negative, possibly due to small sample sizes; the largest number of left-handers in any of these studies was 198 (16). Cortex-wide screening using atlas-defined regions has also not shown robust associations with hand preference (23, 24), even in as many as 608 left-handers versus 7,243 right-handers. One possibility is that brain anatomical correlates of handedness may be too focal to be captured by common atlas-defined parcellations. To this end, atlas-free mapping in a large population sample may provide new insights into how hand preference relates to cerebral cortical structural asymmetry.

Significance

Left-handedness occurs in roughly 10% of people, but whether it involves altered brain anatomy has remained unclear. We measured left to right asymmetry of the cerebral cortex in 28,802 right-handers and 3,062 left-handers. There were small average differences between the two handedness groups in brain regions important for hand control, language, vision, and working memory. Genetic influences on handedness were associated with some of these brain asymmetries, especially of language-related regions. This suggests links between handedness and language during human development and evolution. One implicated gene is *NME7*, which also affects placement of the visceral organs (heart, liver, etc.) on the left to right body axis—a possible connection between brain and body asymmetries in embryonic development.

Author contributions: Z.S., A.P., A.C.-C., J.M.R., R.W., M.J., S.E.F., F.C., and C.F. designed the research; Z.S., A.P., and D.S. analyzed data; Z.S., A.P., D.S., A.C.-C., J.M.R., R.W., M.J., S.E.F., F.C., and C.F. wrote the paper; Z.S. performed visualization; M.J., S.E.F., F.C., and C.F. acquired funding; and F.C. and C.F. provided direction and supervision.

The authors declare no competing interest.

This article is a PNAS Direct Submission. M.C.C. is a guest editor invited by the Editorial Board.

See online for related content such as Commentaries.

[1]To whom correspondence may be addressed. Email: Clyde.Francks@mpi.nl.

This article contains supporting information online at http://www.pnas.org/lookup/suppl/doi:10.1073/pnas.2113095118/-/DCSupplemental.

Published November 16, 2021.

The most statistically robust association of handedness with brain anatomy reported to date is altered average whole-hemispheric skew, or "torque," in the horizontal and vertical planes found in 35,338 right-handed versus 3,712 left-handed adults from the UK Biobank (25). However, an association of whole-hemispheric torque with handedness does not identify specific brain regional asymmetries linked to this behavioral trait. Associations of left-handedness have also been reported with increased functional connectivity between left and right language networks in roughly 9,000 UK Biobank individuals (26) in an analysis of resting-state functional MRI data. The asymmetry of intrahemispheric functional connectivity during the resting state has also been associated with hand preference (27). The left hemisphere is dominant for language in more than 95% of the right-handed population but in only around 70% of the left-handed population, which suggests possible developmental and evolutionary relationships between these two functional asymmetries (28–32).

In the present study, we mapped cerebral cortical structural asymmetry with respect to hand preference using a large sample and an atlas-free approach: 28,802 adult right-handers and 3,062 left-handers from the UK Biobank measured for asymmetries of cortical surface area and thickness at each of 163,842 vertices in each hemisphere, before down sampling the asymmetry maps to 8,681 vertices to test associations with hand preference. Vertex-wise correspondence between the left and right hemispheres was achieved through resampling each individual's cortical surface model to a symmetrical template created by interhemispheric coregistration (33, 34). This surface-based registration approach aligns cortical folding patterns across individuals and both hemispheres.

Using these data, we first aimed to identify specific clusters of vertices where cortical surface area or thickness asymmetries differed significantly at the group level between right and left-handers, for a uniquely well-powered and precision mapping analysis of the cortical correlates of hand preference. We then used meta-analyzed functional MRI (fMRI) data to annotate the cognitive and behavioral functions of the implicated cortical regions based on independent studies.

Handedness is a partly heritable trait with estimates of the heritability due to common genetic polymorphisms ranging from 1.2 to 5.9% across different large-scale studies and cohorts (35, 36) and around 25% in twin-based studies (37). Recent large-scale genome-wide association studies (GWAS) have made progress on the identification of genetic influences on handedness (26, 35, 36) and separately also on brain structural asymmetry (11). However, no study has previously investigated shared genetic influences on handedness and its specific cortical structural correlates. Using genome-wide genotype data for single-nucleotide polymorphisms (SNPs) in the UK Biobank individuals, we tested the SNP-based heritabilities of the cortical asymmetry measures at each regional cluster associated with hand preference, and also the genetic correlations between these regional cortical asymmetries. We then tested if polygenic disposition to left-handedness was associated with the specific cortical regional asymmetries that are associated with this behavioral trait, including the use of causal mediation analyses. In addition, we tested 39 individual SNPs in relation to the asymmetries of these cortical regions—the SNPs were previously implicated in left-handedness by a GWAS of 1,766,671 individuals (36). Together, these analyses would reveal numerous insights into the biology of gene–brain–behavioral links involving human hand preference.

Results

High-Resolution Mapping of Hand Preference in Relation to Cerebral Cortical Asymmetry in 31,864 Individuals. For each of 28,802 right-handed and 3,062 left-handed adult individuals from the UK Biobank, we generated a cortical surface area asymmetry map and a cortical thickness asymmetry map, in which asymmetries were ultimately measured for each of 8,681 vertices across the cortical surface using an asymmetry index: AI = (Left − Right)/((Left + Right)/2) (*SI Appendix*, Figs. S1 and S2 and see *Materials and Methods*).

For cortical surface area asymmetries, we found eight significant clusters (cluster-level corrected $P < 0.05$) where left-handers differed on average from right-handers: three on the anterior insula (most significant peak t-value = 4.98, P value = 6.55×10^{-7}), one on the precentral gyrus (peak t = 4.35, $P = 1.34 \times 10^{-5}$), three in the anterior middle cingulate cortex (most significant peak t = 4.43, $P = 9.32 \times 10^{-6}$), and one on the inferior temporal/fusiform cortex (peak t = 4.74, $P = 2.13 \times 10^{-6}$; Fig. 1 and *SI Appendix*, Fig. S3 and Table S1). The most anterior of the insula clusters also extended onto the neighboring pars triangularis and pars orbitalis (Fig. 1 and *SI Appendix*, Fig. S3).

For cortical thickness asymmetries, there were two clusters where left-handers differed on average from right-handers (cluster-level corrected $P < 0.05$): one on the postcentral gyrus (peak t = 4.05, $P = 4.12 \times 10^{-5}$) and one on the inferior occipital gyrus (peak t = 4.09, $P = 4.39 \times 10^{-5}$; Fig. 2 and *SI Appendix*, Fig. S4 and Table S1).

Strikingly, for all surface areas and thickness asymmetries within these significant clusters, left-handers showed lower average asymmetry indexes than right-handers: in other words, if a cluster had an average rightward asymmetry in right-handers, it had a stronger average rightward asymmetry in left-handers, and if a cluster had an average leftward asymmetry in right-handers, it had a weaker average leftward asymmetry in left-handers (*SI Appendix*, Fig. S5 and Table S1). These data indicate that left-handedness at the group level is associated with a relative shift of neural resources to the dominant right hemisphere for hand motor control, within all of the significant handedness-associated cortical clusters. The unilateral hemispheric group-average effects corresponding these clusters are in *SI Appendix*, Table S2.

Functional Annotation of Cortical Regional Asymmetries Linked to Hand Preference. We used meta-analyzed fMRI activation data from 14,371 studies compiled within the Neurosynth database (38) to annotate our handedness-associated structural asymmetry maps with cognitive and behavioral functions (see *Materials and Methods*).

The clusters with altered average surface area asymmetries in left-handedness are especially activated by tasks involving executive functions, language and reading, mood, and pain perception (Fig. 3 and *SI Appendix*, Table S3). The language-related annotations such as "word, phonological, orthographic, reading, and language" were likely contributed by the anterior insula and fusiform clusters in particular (Fig. 1 and *SI Appendix*, Fig. S3): clusters 2 and 8 on the anterior insula and cluster 1 on the fusiform cortex overlap with regions identified as being conjointly and left-asymmetrically activated in three sentence-level language task contrasts (39). Hemispheric language dominance is known to associate with hand preference, as atypical right-hemispheric language dominance is more frequent in left-handed than right-handed people (29, 40).

We found that clusters with altered cortical thickness asymmetries in left-handedness are especially activated by tasks involving hand and finger movement as well as somatosensory and tactile tasks (Fig. 3 and *SI Appendix*, Table S3), likely contributed in particular by the postcentral gyrus cluster. The top functional terms were "movements, hand, execution, finger, action, motor, and motion" (Fig. 3 and *SI Appendix*, Table S3). These functional annotations based on independent fMRI data serve as a strong validation of the cortical thickness asymmetry

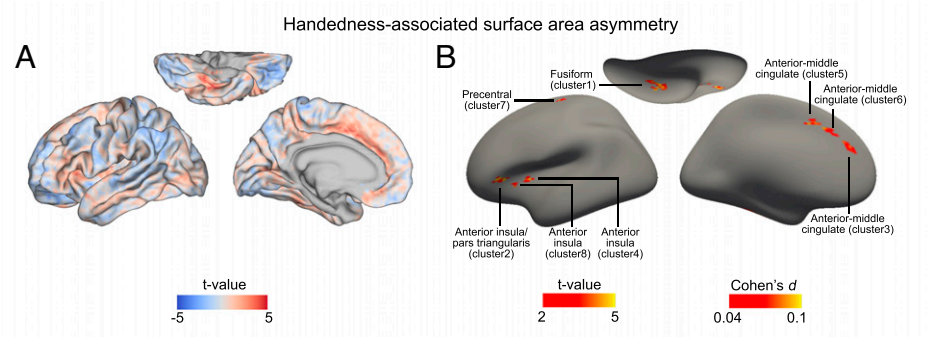

Fig. 1. Handedness-associated cortical surface area asymmetries. (*A*) Group average differences of cortical surface area asymmetry between 28,802 right-handers and 3,062 left-handers shown for the whole cortex, without a threshold for significance. Red color indicates a lower asymmetry index in left-handers (weaker average leftward or stronger average rightward asymmetry in left-handers compared to right-handers). Blue indicates a higher asymmetry index in left-handers (stronger average leftward or weaker average rightward asymmetry in left-handers compared to right-handers). (*B*) Regional clusters with significant group average differences of surface area asymmetry between 28,802 right-handers and 3,062 left-handers. There were eight clusters that survived multiple testing correction (vertex-wise $P < 0.001$; cluster-wise $P < 0.05$). For all clusters, the effects were positive (weaker average leftward or stronger average rightward asymmetry in left-handers compared to right-handers). The clusters are shown on an inflated cortical surface model to visualize effects within folded regions. See also *SI Appendix*, Fig. S3, which shows the same maps against Brodmann regional atlas boundaries, for reference.

associations with left-handedness that we observed (Fig. 3 and *SI Appendix*, Table S3). There were also numerous visual system–related functional annotations for the regions with altered cortical thickness asymmetries in left-handedness (*SI Appendix*, Table S3), likely contributed especially by the inferior occipital cluster (Fig. 2 and *SI Appendix*, Fig. S4).

The term "motor" was annotated to the clusters showing altered surface area asymmetry and to those showing altered thickness asymmetry in left-handedness (*SI Appendix*, Table S3), again supporting the validity of these anatomy–handedness associations.

Genetic Disposition to Left-Handedness Associates with Specific Cortical Asymmetries That Are Altered in Left-Handedness. We made use of UK Biobank genome-wide genotype data to calculate the SNP-based heritabilities (41) of the cortical asymmetry measures, for each separate cluster that was associated with hand preference (*Materials and Methods* and *SI Appendix*, Table S4). These heritability values indicate the extent to which common genetic variation across the genome influences interindividual variation in each of the left-handedness–associated cortical regional asymmetries. The surface area asymmetries of the fusiform cluster, the three anterior insular clusters, and one anterior middle cingulate cluster were weakly but significantly heritable after false discovery rate (FDR) correction at 0.05, with pointwise heritability estimates ranging from 3.1 to 6.3% (Fig. 4 and *SI Appendix*, Table S4). The surface area asymmetry of the precentral gyrus cluster was not significantly heritable (pointwise heritability 0.0, $P = 0.5$). Likewise, the cortical thickness asymmetries associated with left-handedness were not significantly heritable, with pointwise estimates no greater than 1.4% (lowest $P = 0.10$) (Fig. 4 and *SI Appendix*, Table S4).

Genetic correlation analysis indicated that the surface area asymmetries of the three anterior insula clusters were influenced by largely the same genetic variants across the genome, with significant pairwise genetic correlations from 0.85 to 1.0, whereas other pairwise genetic correlations between heritable regional asymmetries were weaker (see phenotypic and genetic correlations in *SI Appendix*, Tables S5 and S6).

From an independent set of 272,673 right-handed and 33,704 left-handed individuals of the UK Biobank who were not overlapping and unrelated to those with brain image data, we derived effect sizes for the association of each SNP across the genome with hand preference (see *Materials and Methods*). We then applied these SNP-wise effects in mass combination to the 28,802 right-handed and 3,062 left-handed individuals that had

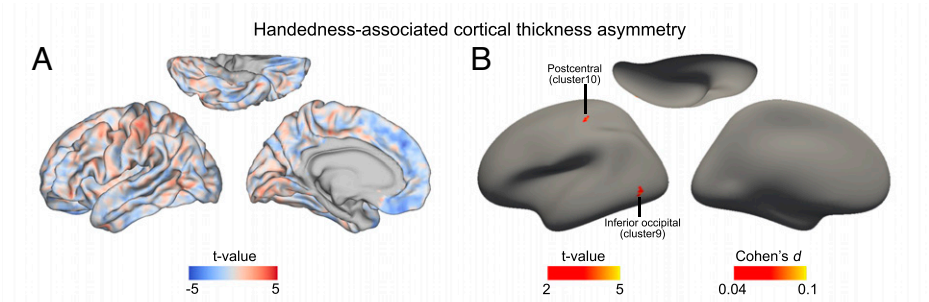

Fig. 2. Handedness-associated cortical thickness asymmetries. (*A*) Group average differences of cortical thickness asymmetry between 28,802 right-handers and 3,062 left-handers shown for the whole cortex, without a threshold for significance. Red color indicates a lower asymmetry index in left-handers (weaker average leftward or stronger average rightward asymmetry in left-handers compared to right-handers). Blue indicates a higher asymmetry index in left-handers (stronger average leftward or weaker average rightward asymmetry in left-handers compared to right-handers). (*B*) Regional clusters with significant group average differences of cortical thickness asymmetry between 28,802 right-handers and 3,062 left-handers. There were two clusters that survived multiple testing correction (vertex-wise $P < 0.001$; cluster-wise $P < 0.05$). For both clusters, the effects were positive (weaker average leftward or stronger average rightward asymmetry in left-handers compared to right-handers). The clusters are shown on an inflated cortical surface model to visualize effects within folded regions. See also *SI Appendix*, Fig. S4, which shows the same maps against Brodmann regional atlas boundaries, for reference.

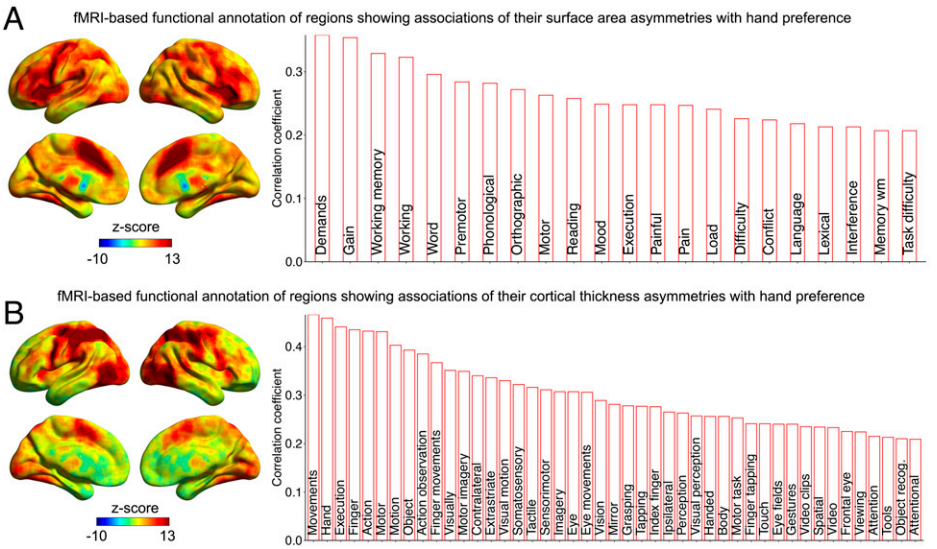

Fig. 3. Functional annotation of regions that show altered asymmetry in left-handedness. Functional annotation based on meta-analyzed fMRI data for clusters showing altered surface area asymmetry (*A*) and cortical thickness asymmetry (*B*) in left-handedness. (*Left*) Coactivation maps for the handedness-associated clusters derived from the "decoder" function of Neurosynth (higher z-scores indicate greater coactivation). (*Right*) Cognitive terms associated with the coactivation maps for handedness-associated clusters. Only terms with correlations >0.2 between their meta-analytic activation maps and the coactivation maps for handedness-associated clusters are shown. See also *SI Appendix*, Table S3.

genetic and brain image data for the present study, in order to quantify their polygenic dispositions to left-handedness, using the PRS-CS software (42). Polygenic disposition to left-handedness was significantly associated with hand preference in this sample as expected (logistic regression beta = 0.12, $P = 6.63 \times 10^{-8}$; see *SI Appendix*, Fig. S6 for more information), as well as cerebral cortical surface area asymmetry within the fusiform cluster (r = −0.02, $P = 0.003$), anterior insula cluster 2 (r = −0.02, $P = 6.59 \times 10^{-4}$) and anterior insula cluster 4 (r = −0.02, $P = 9.01 \times 10^{-5}$) after FDR correction at $P < 0.05$ (Fig. 4 and *SI Appendix*, Table S7). Specifically, higher polygenic disposition to left-handedness was associated with increased average rightward asymmetry in the fusiform cluster and decreased average leftward asymmetry in the anterior insula clusters (Fig. 4), consistent with the associations of these regional surface area asymmetries with the left-handedness trait itself. The polygenic disposition to left-handedness was not associated with any other regional cortical asymmetries linked to left-handedness, including the precentral surface area asymmetry cluster and the postcentral thickness asymmetry cluster (Fig. 4 and *SI Appendix*, Table S7).

Separately for the fusiform cluster and each anterior insula cluster that showed association with polygenic disposition to left-handedness, we applied mediation analyses according to two possible causal models: polygenic disposition > asymmetry > handedness and polygenic disposition > handedness > asymmetry (*Materials and Methods*). All of the models showed evidence of both direct and mediated effects (*SI Appendix*, Fig. S7 and Tables S8 and S9).

Individual Genomic Loci Associated with Hand Preference and Its Cerebral Cortical Correlates. A previous GWAS based on 1,766,671 individuals found 41 individual genomic loci that were significantly associated with left-handedness after multiple testing correction over the whole genome (36). In the 28,802 right-handed and 3,062 left-handed individuals with both genetic and brain image data in the present study, we found that 18 of these genomic loci were associated with at least one

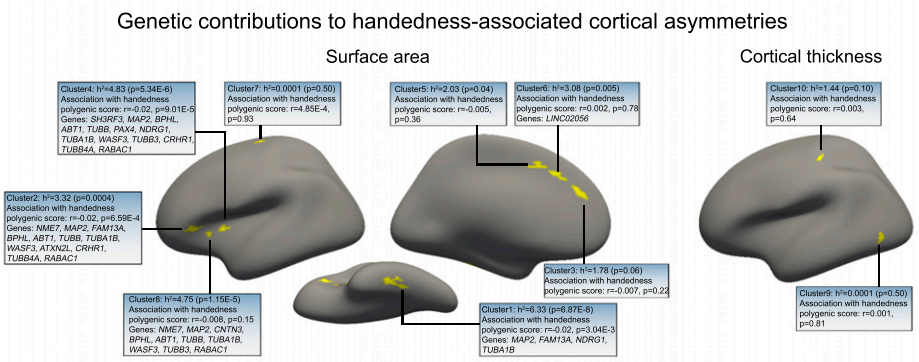

Fig. 4. Genetic influences on hand preference impact some of the cortical asymmetries linked to hand preference. Five clusters of handedness-associated cortical surface area asymmetry showed significant heritabilities after FDR correction (i.e., three clusters in the anterior insular cortex [clusters 2, 4, and 8], one in the fusiform cortex [cluster 1], and one in the anterior middle cingulate cortex [cluster 6]). Other handedness-associated asymmetry clusters were not significantly heritable, including the pre- and postcentral clusters of the sensorimotor cortex (clusters 7 and 10). The associations of cortical asymmetries with polygenic disposition to left-handedness are indicated, as well as individual handedness-associated genes implicated in their variabilities.

of the cortical surface area asymmetry clusters that are linked to left-handedness after FDR correction at 0.05 (Fig. 4 and *SI Appendix*, Table S10). In particular, 17 out of these 18 SNPs were associated with surface area asymmetry of either the fusiform cluster or at least one of the anterior insula clusters (Fig. 4 and *SI Appendix*, Table S10).

The protein-coding genes located nearest to these SNPs in the genome include four that encode tubulin components of microtubules, TUBB, TUBA1B, TUBB3, and TUBB4A, as well as the microtubule-associated proteins MAP2 and NME7. These findings are in line with another recent study which implicated microtubule-related genes in brain structural asymmetry, in that case using atlas-based regional definitions across the whole brain but without considering handedness (11). Recessive mutations in *NME7* cause situs inversus totalis, a rare condition in which the visceral organs (heart, liver, etc.) are reversed in their orientation on the left to right axis (43). Other genes implicated by the present study to affect both handedness and its specific cerebral cortical correlates include *CNTN3*, which mediates cell surface interactions during nervous system development (44), and *ATXN2L*, implicated in macrocephaly by de novo mutation (45).

Discussion

Cerebral Cortical Structural Asymmetry with Respect to Hand Preference. In this study, we mapped cerebral cortical correlates of hand preference in 28,802 right-handed and 3,062 left-handed adults using an atlas-free, cortex-wide approach. This was by far the largest study of this question to date and brings clarity to a long-standing issue in human neuroscience, as previous studies had reported contradictory, equivocal, and/or negative results (see the introduction). Vertex-level mapping allowed us to detect and delineate relatively focal correlates of hand preference on the cortical surface, which may have been concealed in a previous consortium-scale study that used atlas-based regional parcellation—although the total sample size in that study was also smaller (7,243 right-handers and 608 left-handers), which would have affected the statistical power to detect subtle group-average effects (23, 46).

We found that, at the group level, left-handers had an average less leftward/more rightward shift of specific regional cortical surface area or thickness asymmetry than right-handers, distributed in several cortical regions: the fusiform, the anterior insula, the precentral, the postcentral, the anterior middle cingulate, and the inferior occipital cortex. For all of these regions, the average alterations were consistent with a relative shift of neural resources to the right hemisphere that controls the preferred hand in left-handers. Together, the implicated regions suggest a distributed neural network associated with controlling articulation of the preferred hand.

Functional annotation of the regions with altered average surface area asymmetries in left-handers, based on independent fMRI data from 14,371 meta-analyzed studies, pointed to their involvements in executive functions including working memory as well as language and reading, mood, and pain perception. Regarding language, previous studies have found an increase in atypical right-hemisphere language dominance among left-handed people (29, 40) (see the introduction). We found an association between hand preference and surface area asymmetry within the anterior insular cortex/pars triangularis corresponding to core regions of the language network that show left-lateralized activation during sentence-level language tasks (39). The anterior insula has been suggested to be especially important for the establishment of functional language lateralization during development through integrating across social, emotional, and attentional systems when acquiring language early in life (46). We found no significant associations of hand preference with asymmetries of superior temporal or middle temporal cortex, which are also core language network regions (39). Thus, hand preference apparently relates to cortical structural asymmetry of frontal and fusiform language regions in particular, rather than other language network regions that are closer to the auditory cortex of the temporal lobe.

fMRI-based annotation of the cortical regions with altered average thickness asymmetries in left-handers confirmed their involvements in hand sensorimotor functions with top annotations of "movements, hand, execution, finger," and so on. This functional annotation based on independent data provides validation of the group-level cortical asymmetry alterations in left-handedness that we detected. As noted in the introduction, some previous studies targeted the central sulcus as a region of interest and reported altered cortical anatomy there in left-handers, but they were based on small samples and variable methods and measures with conflicting results, such that the findings remained uncertain. Here, we have implicated a specific region of the postcentral gyrus through cortex-wide, atlas-free mapping in a large sample and shown that cortical thickness asymmetry rather than surface area asymmetry is the feature most correlated with hand preference in this region. In contrast, we found that a specific region of precentral "premotor" cortex showed altered average surface area asymmetry in left-handers.

The regions that showed altered average cortical thickness asymmetry in left-handers also received numerous vision-related annotations based on fMRI data, such as "'motor imagery, visual motion, eye movements, visual perception, eye fields," and so on. These annotations were likely driven by the inferior occipital cluster. Left-handers have been reported to show more variable hemispheric involvement than right-handers in visual half-field tasks, which can index lateralized contributions to visual attentional tasks (47). The need for hand–eye coordination during complex manual tasks may drive this relationship. However, the inferior occipital cluster also lies within a language network region that shows left-lateralized activation during sentence-level tasks presented in different modalities (39).

Shared Genetic Influences on Hand Preference and Its Specific Cerebral Cortical Correlates. We found that polygenic disposition to left-handedness was associated with specific handedness-linked asymmetries of surface area in the fusiform and anterior insular cortex. The directions of effect were as expected: higher polygenic disposition to left-handedness–associated with reduced average leftward or increased average rightward surface area asymmetry in these cortical regions—the same as for left-handedness itself. Notably, the regional cortical thickness asymmetries associated with hand preference (i.e., within the postcentral gyrus and inferior occipital cortex) were not significantly heritable and showed no associations with polygenic disposition to left-handedness. Neither did the surface area asymmetry of the precentral gyrus cluster. Therefore, some specific handedness-related cortical asymmetries share genetic influences with hand preference, while others apparently do not, at least to extents that could be detected in the current sample size.

In the adult cross-sectional data of the UK Biobank, it is not possible to establish cause–effect relations unambiguously. Mediation models were compatible with fusiform and anterior insula surface area asymmetries partly mediating the effect of polygenic disposition on hand preference, but also the other way around, i.e. hand preference partly mediating an effect of left-handedness polygenic disposition on these brain asymmetries. Both models are plausible, as brain anatomy may in principle be both causal to behavioral outcomes and shaped plastically by repeated behaviors, or indeed merely correlated because of shared underlying

factors (48). However, the cortical asymmetries that share genetic influences with hand preference seem more likely to be involved in its etiology than those which do not, especially as some of the implicated genes may point to mechanisms of establishing the brain's left to right axis in early development (see discussion of specific genes below). Furthermore, structural asymmetry of the anterior insula—the region with the strongest evidence for shared genetic influences on both its asymmetry and hand preference—is already detectable in the fetal brain (49).

In contrast, nonheritable correlates of hand preference in the adult cortex, including the sensorimotor cortex, may reflect plastic adaptation after the preference is already established developmentally. The lack of heritability of these asymmetries in the adult brain could then reflect their relatively distal relationships to genetically regulated mechanisms of left to right brain axis formation in the embryo. However, left-handedness has shown only limited associations with environmental and early life factors studied so far (50, 51) and is also only weakly to moderately heritable (35–37). This suggests that left-handedness arises largely from random (nonheritable) early developmental variation (52) occurring around a genetically regulated program that is biased toward a right-handed outcome. In other words, the genetically regulated program of asymmetrical brain development appears to give rise to right-handedness with roughly 90% probability and left-handedness with roughly 10% probability, while both interindividual genetic and environmental variation seem to have generally small impacts on these baseline probabilities. In this way, left-handedness might have some brain structural and functional correlates linked to its early development which are neither heritable nor affected by environmental variation.

This study pinpointed individual genomic loci which associate with both hand preference and some of its specific cortical structural correlates. The involvement of microtubule-related genes in human handedness and brain asymmetry suggests a possible mechanism whereby left to right asymmetry of the brain arises in the embryo from cellular chirality (an asymmetrical twisting of cellular shape specified by the cytoskeleton—internal cellular structure composed of protein filaments and microtubules) (11). Such mechanisms have been described with respect to other organs of other invertebrate and vertebrate species and can be organ intrinsic (i.e., arise independently from other developing organs or systems) (53–59). This seems especially pertinent to the brain, as left-hemisphere dominances for hand preference and language do not usually reverse in people with situs inversus totalis (i.e., reversal of the visceral organs on the left-right axis) when caused by genetic mutations which affect primary ciliary components (60–63). Primary cilia play an important role in the establishment of visceral asymmetry, in which the molecular chirality of the axoneme (microtubule-based central strand of the cilium) results in unidirectional ciliary motion within the embryonic node (64, 65).

In this context, it is especially notable that our data implicated *NME7* in affecting both hand preference and handedness-associated cortical surface area asymmetries. Recessive mutations in this gene cause situs inversus totalis but without primary ciliary dyskinesia (i.e., ciliary function remains largely or wholly unaffected even while the visceral organs become reversed) (43). The functions of this gene are not well understood, but it is known to associate with γ-tubulin and the ciliary axoneme (43); thus, it has potential functions that involve the cilium but also the microtubule cytoskeleton more generally. *NME7* provides a possible genetic link between brain and body asymmetry via as-yet-unidentified mechanisms which do not necessarily involve ciliary dysfunction and the nodal pathway of visceral laterality formation (60). All of the genes implicated here to affect both hand preference and its cerebral cortical correlates should be studied with gene-functional approaches, such as in cellular models and knockout mice, to understand their roles in affecting brain functional and structural laterality.

Limitations. Vertex-wise mapping of asymmetry assumes that high-resolution correspondence can be achieved between contralateral vertices in the two hemispheres. For the most part the method appears to have worked well, insofar as it distinguished some regions of association with hand preference that make sense on a priori grounds, such as the sensorimotor cortex of the pre- and postcentral sulcus and language-related regions. However, we found it necessary to exclude a region surrounding the boundary with subcortical structures at the center of the brain (affecting entorhinal, parahippocampal, and cingulate regions; *SI Appendix*, Fig. S8), where extreme vertex-wise asymmetry values were present in many individuals (see *Materials and Methods*). This may indicate an artifact that involves extreme warping for this region to fit the symmetrical template.

The limitation of the UK Biobank cross-sectional data for making causal inferences from associations was already mentioned in the section *Shared Genetic Influences on Hand Preference and Its Specific Cerebral Cortical Correlates*. In addition, the UK Biobank is a volunteer cohort of middle-aged to older adults and therefore not fully representative of the population, with generally superior health and socioeconomic circumstances for this age range, and greater female participation (66). Higher risk for psychiatric disorders has been suggested to reduce participation in cohort studies (67), and we have previously found evidence for this in the UK Biobank (68).

In this study, we linked genetic, brain structural, and behavioral data and made use of independent, meta-analyzed fMRI data to understand the functions of the implicated sets of cortical regions. Future studies of hand preference in large datasets may seek to integrate more aspects of brain structure and function from the same individuals into the analyses, including task-based or resting-state fMRI and diffusion tensor imaging data on white matter structural connectivity.

The assessment of hand preference was by a simple questionnaire in which individuals could choose between four options: right-handed, left-handed, use both hands equally, or prefer not to answer. We found the "both hands" category to be relatively unreliable over repeat visits (*Materials and Methods*), which led us to use a binary left/right variable for the purposes of this study. Simple assessments such as this have been shown to capture an inherent dichotomy in hand preference that is also revealed by more quantitative, multi-item questionnaires (69). However, brain–behavior association results may have been different if using performance-based hand skill measures or semiquantitative multi-item handedness ratings, and ambidextrous people may form a somewhat distinct category with respect to behavioral and brain correlates (70, 71).

This study examined average group differences in cerebral cortical asymmetry between left- and right-handers. Future studies may consider the possibility that left-handedness associates with increased variability in terms of brain structure and function.

Summary. This study used a symmetrical surface template to achieve atlas-free mapping of cerebral cortical asymmetry with respect to hand preference in an unprecedented sample size. Detailed and statistically reliable maps of the cortical correlates of human hand preference were produced, resolving a long-standing issue in human neuroscience. The implicated regions are especially involved in executive, language, motor, and visual functions. Across all the regions, the data uniformly indicated a less leftward/more rightward shift of neural resources in left-handers compared to right-handers, consistent with right-hemispheric control of the left hand. Hand preference was

genetically associated with the asymmetries of frontal and fusiform language network regions, supporting developmental and evolutionary links between hand preference and language. Various other regional asymmetries associated with hand preference were not heritable and may reflect plastic changes in support of hand preference, including those of the primary sensorimotor cortex. Specific genes found to affect both hand preference and its cerebral cortical correlates included microtubule-related genes, one of which—*NME7*—provides a potential mechanistic link between brain and visceral asymmetries, which might not involve impaired ciliary function. This study provides an example of how linking across human genetics, brain structure, and behavior in large datasets can provide tangible new knowledge, as well as mechanistic and developmental hypotheses for future research on typical and atypical human brain function.

Materials and Methods

Participants. This study was conducted under UK Biobank application 16066, with Clyde Francks as principal investigator. The UK Biobank is a general adult population cohort (72, 73). The UK Biobank received ethical approval from the National Research Ethics Service Committee North West - Haydock (reference 11/NW/0382), and all of their procedures were performed in accordance with the World Medical Association guidelines. Informed consent was obtained for all participants.

Imaging genetics dataset. We used the UK Biobank neuroimaging data (74, 75) released in February 2020 together with the genotype data from the same participants. To achieve a sufficiently high degree of homogeneity for the genetic analyses, we restricted the sample to participants with "White British ancestry" defined by Bycroft et al. ("in.white.British.ancestry.subset") (72). We excluded subjects with a mismatch of their self-reported and genetically inferred sex, with putative sex chromosome aneuploidies, or who were outliers based on heterozygosity (principal component corrected heterozygosity > 0.19) and genotype missingness (missing rate > 0.05) (72). We randomly excluded one subject from each pair with a kinship coefficient >0.0442 as defined by the UK Biobank (72).

Handedness was assessed by a touchscreen question with four choices: right-handed, left-handed, use both right and left hands equally, and prefer not to answer (UK Biobank field: 1707). We previously found that those indicating mixed handedness (roughly 2% of all individuals) had a high rate (41%) of changing their answers over repeat visits to the assessment centers, whereas those indicating either right-handedness or left-handedness at their first visit had consistency rates >97% on subsequent visits (31, 50). We therefore excluded mixed handers and focused only on those indicating either right- or left-handedness during their first visit.

These steps resulted in a final sample of 31,864 participants comprising 28,802 right-handers and 3,062 left-handers. The age range of these participants was from 45 to 81 y (mean 63.75), and 15,064 were male and 16,800 female.

Genome-wide screening dataset to obtain SNP-wise effect sizes for association with hand preference. These additional UK Biobank individuals had genetic and handedness data but not brain image data. We applied the same genetic and handedness exclusion criteria as in the section *Imaging genetics dataset* with the extra requirement that none of these individuals should have a kinship coefficient >0.0442 with any of the individuals in the imaging genetic dataset. This yielded 272,673 right-handed and 33,704 left-handed participants not overlapping and unrelated to the set with brain imaging data.

MRI Processing. Brain image data were derived from T1-weighted MRI scans (Siemens Skyra 3 Tesla MRI with 32-channel radio frequency receive head coil). We started from the Freesurfer 6.0 (76) "recon-all" cortical reconstructions generated by the UK Biobank imaging team (UK Biobank data field 20263, first imaging visit) but did not make use of image-derived phenotypes released by that team. Rather, the cortical thickness and surface area maps of both hemispheres of each individual were resampled into a standard symmetrical space created using interhemispheric coregistration (fsaverage_sym) (33), with 163,842 vertices per hemisphere (*SI Appendix*, Fig. S9). This process required roughly 10 wk of processing on 12 cluster server nodes running in parallel and precisely aligned morphometry features between the two hemispheres to achieve vertex-wise correspondence. Separately for surface area and thickness maps, asymmetry for each left–right-matched pair of vertices in each participant was calculated according to the asymmetry index AI = (left − right)/((left + right)/2). The asymmetry maps for surface area and thickness of each individual were then down sampled to the left-hemisphere of template "fsaverage5" (10,242 vertices per hemisphere; *SI Appendix*, Fig. S9).

We noticed that many individuals had extreme values of asymmetry in a region wrapping around the boundary with subcortical structures near the center of the brain (*SI Appendix*, Fig. S8), which likely arises from a registration artifact. For this region, we excluded any vertices from all individuals when they had surface area |AI|>1 in at least 1,000 (~3%) individuals (*SI Appendix*, Fig. S8) (i.e., excluded from subsequent analyses of both surface area and cortical thickness asymmetries). This left 8,681 vertex-wise asymmetry measures per individual spanning the majority of the cerebral cortex.

Mapping Cortical Asymmetry Correlates of Hand Preference. For each vertex, brain asymmetry differences between left- and right-handers were examined by two-sample *t* tests separately for surface area and cortical thickness while controlling for continuous covariates: age when attended assessment center (field 21003–2.0), quadratic age (age − mean_age)^2, scanner position parameters (X, Y, and Z: fields 25756–2.0, 25757–2.0, and 25758–2.0), T1 signal-to-noise ratio (field 25734–2.0), and T1 contrast-to-noise ratio (field 25735–2.0) together with two categorical covariates: assessment center (field 54–2.0) and sex (field 31–0.0). Significant clusters were determined by the random field theory method at a cluster-corrected level of $P < 0.05$ (clusters forming with vertex-level $P < 0.001$) to minimize the likelihood of false positive results using the SurfStat toolbox (https://www.math.mcgill.ca/keith/surfstat/). Each cluster identified in this way has a peak vertex and additional contiguous vertices, with cluster-wise significance assessed against a random field with the same spatial correlation as the real map.

As a post hoc analysis, we also examined the unilateral effects corresponding to clusters with altered asymmetry in left-handers. Specifically, for each hemisphere and individual, we calculated the mean unilateral value across all vertices within each significant cluster and compared the differences between left- and right-handers by two-sample *t* tests while controlling for the same covariates mentioned above.

Functional Annotation of Cortical Regions Showing Altered Asymmetry in Left-Handers. We made use of the Neurosynth database (38), a platform for large-scale automated synthesis of task-based fMRI data. This database defines brain-wide activation maps corresponding to specific cognitive or behavioral task terms using meta-analyzed functional activation maps from studies referring to those terms (38). At the time of accessing the database, it included 1,307 maps representing activation patterns corresponding to 1,307 cognitive or behavioral terms from 14,371 human neuroimaging studies. We created one bilateral mask in MNI152 standard space by labeling all clusters showing altered average surface area asymmetry in left-handers, and another bilateral mask in Montreal Neurological Institute (MNI) standard space that comprised all clusters showing altered average cortical thickness asymmetry in left-handers. This was achieved through applying the "mri_surf2vol" function in Freesurfer to the down-sampled, handedness-associated asymmetry cluster maps (defined in left hemisphere fsaverage5 surface space) and then identifying the mirrored voxels (based on the midline of left and right hemisphere) corresponding to these clusters in the right of the symmetrical standard space, to define masks with bilaterally labeled voxels.

These masks were then used separately as input to identify relevant cognitive and behavioral terms through the "decoder" function of the Neurosynth database. This tool first creates a coactivation map for each input mask based on all activation data in the database and then tests each term-specific activation map for spatial correlation with the coactivation map. Cognitive terms with correlations >0.2 are reported while excluding anatomical terms, nonspecific terms (e.g., "Tasks"), and one from each pair of virtually duplicated terms (such as "Words" and "Word"). This tool does not employ inferential statistical testing but rather ranks cognitive and behavioral terms according to the correlations of their meta-analyzed activation maps with the coactivation map that corresponds to a user-defined input mask.

Heritabilities and Genetic Correlations of Cortical Asymmetries Associated with Hand Preference. From the imputed SNP genotype data released by the UK Biobank (March 2018), 9,516,135 autosomal variants with minor allele frequencies > 1%, INFO (imputation quality) score > 0.7 and Hardy–Weinberg equilibrium $P > 1 \times 10^{-7}$ were used to build a genetic relationship matrix using the Genome-wide Complex Trait Analysis (GCTA) software (77) (version 1.93.0beta). Specifically for analyses using GCTA, we further excluded one random participant from each pair having a kinship coefficient higher than 0.025 based on the calculated genetic relationship matrix (this analysis is particularly sensitive to higher levels of relatedness), resulting in 29,973 participants for this particular analysis (27,083 right-handed and 2,890 left-handed). Genome-

based restricted maximum likelihood (GREML) analysis using GCTA (77) was used to estimate the SNP-based heritability for each cluster that showed altered asymmetry in left-handedness (using the mean asymmetry index across all vertices within each cluster), controlling for the abovementioned covariates [i.e., age, (age–mean_age)^2, scanner position parameters, T1 signal-to-noise ratio, T1 contrast-to-noise ratio, assessment center, and sex] plus an additional binary covariate for genotyping array and the first ten genetic principal components capturing population genetic diversity (UK Biobank field ID: 22009–0.1∼22009–0.10) (72) and then applying FDR 0.05 across the 10 clusters. Bivariate GREML analysis (78) was used to estimate genetic correlations between pairs of significantly heritable cluster-wise asymmetries.

Polygenic Disposition to Left-Handedness. In 272,673 right-handers and 33,704 left-handers who were not overlapping and unrelated to those with brain image data (see *Genome-wide screening dataset to obtain SNP-wise effect sizes for association with hand preference*), we again excluded genetic variants with minor allele frequencies < 1%, INFO score ≤ 0.7, and Hardy–Weinberg equilibrium P value ≤ 10^{-7}. We then carried out an autosome-wide association scan for right- versus left-handedness under an additive genetic model with covariates for year of birth, sex, genotyping array, and the first 10 genetic principal components capturing population genetic diversity, using BGENIE (v1.2) (72). SNP-wise effects on left-handedness disposition from this sample were then applied in mass combination to the 28,802 right-handers and 3,062 left-handers with post-quality-control imaging and genetic data (see *Imaging genetics dataset*) to estimate their polygenic dispositions to left-handedness, using the PRS-CS software (42). This method uses a high-dimensional Bayesian regression framework to estimate posterior effect sizes of SNPs and has shown superior prediction statistics compared to approaches based on clumping by linkage disequilibrium and P value thresholding (79). In total, effect sizes of 1,103,636 SNPs spanning the autosomes were used based also on their presence in the 1,000 Genomes project European-descent dataset from where PRS-CS obtains its linkage disequilibrium information (80). We used default parameters and the recommended global effect size shrinkage parameter phi = 0.01. The handedness polygenic scores in the imaging genetic dataset were z-standardized for subsequent analyses (*SI Appendix*, Fig. S6).

We first tested whether polygenic disposition to left-handedness was associated with hand preference in the 28,802 right-handers and 3,062 left-handers using logistic regression with hand preference as the outcome variable and covariates of age, (age–mean_age)^2, genotyping array, the first 10 genetic principal components (see *Heritabilities and Genetic Correlations of Cortical Asymmetries Associated with Hand Preference*), and sex.

We then extracted the mean asymmetry index over all vertices within each separate cluster that showed association of its asymmetry with left-handedness (eight clusters for surface area asymmetry, two for thickness asymmetry). Separately for each cluster's mean asymmetry, we performed Pearson correlation analysis with polygenic disposition to left-handedness across individuals while controlling for the same covariates as in the SNP-based heritability analysis (see *Heritabilities and Genetic Correlations of Cortical Asymmetries Associated with Hand Preference*) and applying FDR correction at 0.05 across the 10 clusters tested.

For the asymmetry clusters that were significantly associated with polygenic disposition to left-handedness, we then applied the "mediation" toolbox in R https://www.rdocumentation.org/packages/mediation/versions/4.5.0 using the same covariates and bootstrapping 1,000 times in order to test causal mediation models framed with respect to either polygenic disposition > asymmetry > handedness or polygenic disposition > handedness > asymmetry separately for each cluster's mean asymmetry.

Imaging Genetic Analysis of Individual Loci Associated with Left-Handedness. A previous genome-wide association scan for left- versus right-handedness carried out in 1,766,671 individuals reported 41 individually significant genomic loci after correction for multiple testing across the whole genome (36). There were genotype data for 38 of these SNPs in the 28,802 right-handers and 3,062 left-handers of the imaging genetic sample in the present study, and we identified a proxy SNP for one more of these SNPs [rs11265393 as a proxy for rs66513715 with linkage disequilibrium r-squared of 1 in European-descent data according to LDproxy (81)]. We tested each of these 39 SNPs for association with each of the significantly heritable, cortical cluster-wise asymmetries (averaged over all vertices separately within each cluster) that showed alterations in left-handers using an additive model in BGENIE (v1.2) (72) with the same covariates as the heritability analysis (see *Heritabilities and Genetic Correlations of Cortical Asymmetries Associated with Hand Preference*). All 39 SNPs had imputation quality (INFO) scores > 0.7. We applied the FDR correction at 0.05 to control multiple testing over all of these SNP-cluster combinations.

Note that the previous GWAS of left- versus right-handedness based on 1,766,671 individuals (36) included the UK Biobank participants and therefore also included the participants with brain image data, although the brain image data were not used in that study. The sample overlap meant that we could not use those genome-wide, SNP-wise effect size estimates to calculate polygenic disposition to left-handedness in the current study, as the genome-wide screening and target datasets must not overlap for polygenic scoring analysis. In addition, the SNP-wise effect sizes have not been made publicly available from the GWAS of 1,766,671 individuals (36).

Data Availability. The primary data used in this study are available via the UK Biobank website (https://www.ukbiobank.ac.uk). Four Freesurfer-format (.mgh) cortical effect maps produced by this study are available for download (82): population average cortical surface area asymmetry, population average cortical thickness asymmetry, handedness group average differences in cortical surface area asymmetry, and handedness group average differences in cortical thickness asymmetry.

ACKNOWLEDGMENTS. This research was funded by the Max Planck Society and Grant 054-15-101 from the Netherlands Organization for Scientific Research and Grant 15-HBPR-0001-03 from the French National Research Agency (the latter two grants were components of the FLAG-ERA consortium project "MULTI-LATERAL," a Partner Project to the European Union's Flagship Human Brain Project). This research was conducted using the UK Biobank resource under application no. 16066 with C.F. as the principal applicant. Our study made use of data generated by an image-processing pipeline developed and run on behalf of UK Biobank. The funders had no role in study design, data collection and analysis, the decision to publish, or the preparation of the manuscript. Many thanks to Nathalie Tzourio-Mazoyer and Bernard Mazoyer for their founding roles in the collaborative work that led to this study, and to Chris McManus for helpful comments on the manuscript.

1. S. Coren, C. Porac, Fifty centuries of right-handedness: The historical record. *Science* **198**, 631–632 (1977).
2. C. Faurie, M. Raymond, Handedness frequency over more than ten thousand years. *Proc. Biol. Sci.* **271** (suppl. 3), S43–S45 (2004).
3. I. C. McManus, "The history and geography of human handedness" in *Language Lateralization and Psychosis*, I. E. C. Sommer, R. S. Kahn, Eds. (Cambridge University Press, Cambridge, 2009), pp. 37–58.
4. M. Papadatou-Pastou *et al.*, Human handedness: A meta-analysis. Psychol. *B*ull. **146**, 481–524 (2020).
5. I. B. Perelle, L. Ehrman, An international study of human handedness: The data. *Behav. Genet.* **24**, 217–227 (1994).
6. R. M. Willems, L. Van der Haegen, S. E. Fisher, C. Francks, On the other hand: Including left-handers in cognitive neuroscience and neurogenetics. *Nat. Rev. Neurosci.* **15**, 193–201 (2014).
7. P. G. Hepper, G. R. McCartney, E. A. Shannon, Lateralised behaviour in first trimester human foetuses. *Neuropsychologia* **36**, 531–534 (1998).
8. P. G. Hepper, D. L. Wells, C. Lynch, Prenatal thumb sucking is related to postnatal handedness. *Neuropsychologia* **43**, 313–315 (2005).
9. C. G. F. de Kovel, S. N. Lisgo, S. E. Fisher, C. Francks, Subtle left-right asymmetry of gene expression profiles in embryonic and foetal human brains. *Sci. Rep.* **8**, 12606 (2018).
10. C. Francks, Exploring human brain lateralization with molecular genetics and genomics. *Ann. N. Y. Acad. Sci.* **1359**, 1–13 (2015).
11. Z. Sha *et al.*, The genetic architecture of structural left-right asymmetry of the human brain. *Nat. Hum. Behav.* **5**, 1226–1239 (2021).
12. S. Ocklenburg *et al.*, Epigenetic regulation of lateralized fetal spinal gene expression underlies hemispheric asymmetries. *eLife* **6**, e22784 (2017).
13. M. Papadatou-Pastou, D.-M. Tomprou, Intelligence and handedness: Meta-analyses of studies on intellectually disabled, typically developing, and gifted individuals. *Neurosci. Biobehav. Rev.* **56**, 151–165 (2015).
14. P. Markou, B. Ahtam, M. Papadatou-Pastou, Elevated levels of atypical handedness in autism: Meta-analyses. *Neuropsychol. Rev.* **27**, 258–283 (2017).
15. M. Hirnstein, K. Hugdahl, Excess of non-right-handedness in schizophrenia: Meta-analysis of gender effects and potential biases in handedness assessment. *Br. J. Psychiatry* **205**, 260–267 (2014).
16. D. Marie *et al.*, Descriptive anatomy of Heschl's gyri in 430 healthy volunteers, including 198 left-handers. *Brain Struct. Funct.* **220**, 729–743 (2015).
17. K. Amunts *et al.*, Asymmetry in the human motor cortex and handedness. *Neuroimage* **4**, 216–222 (1996).
18. Z. Y. Sun *et al.*, The effect of handedness on the shape of the central sulcus. *Neuroimage* **60**, 332–339 (2012).
19. A. L. Foundas, K. Hong, C. M. Leonard, K. M. Heilman, Hand preference and magnetic resonance imaging asymmetries of the central sulcus. *Neuropsychiatry Neuropsychol. Behav. Neurol.* **11**, 65–71 (1998).

20. P.-Y. Hervé, F. Crivello, G. Perchey, B. Mazoyer, N. Tzourio-Mazoyer, Handedness and cerebral anatomical asymmetries in young adult males. *Neuroimage* **29**, 1066–1079 (2006).
21. H. Steinmetz, J. Volkmann, L. Jäncke, H.-J. Freund, Anatomical left-right asymmetry of language-related temporal cortex is different in left- and right-handers. *Ann. Neurol.* **29**, 315–319 (1991).
22. C. D. Good *et al.*, Cerebral asymmetry and the effects of sex and handedness on brain structure: A voxel-based morphometric analysis of 465 normal adult human brains. *Neuroimage* **14**, 685–700 (2001).
23. X. Z. Kong *et al.*, ENIGMA Laterality Working Group, Mapping cortical brain asymmetry in 17,141 healthy individuals worldwide via the ENIGMA Consortium. *Proc. Natl. Acad. Sci. U.S.A.* **115**, E5154–E5163 (2018).
24. T. Guadalupe *et al.*, Differences in cerebral cortical anatomy of left- and right-handers. *Front. Psychol.* **5**, 261 (2014).
25. X.-Z. Kong *et al.*, Large-scale phenomic and genomic analysis of brain asymmetrical skew. *Cereb. Cortex* **31**, 4151–4168 (2021).
26. A. Wiberg *et al.*, Handedness, language areas and neuropsychiatric diseases: Insights from brain imaging and genetics. *Brain* **142**, 2938–2947 (2019).
27. M. Joliot, N. Tzourio-Mazoyer, B. Mazoyer, Intra-hemispheric intrinsic connectivity asymmetry and its relationships with handedness and language lateralization. *Neuropsychologia* **93**, 437–447 (2016).
28. M. C. Corballis, From mouth to hand: Gesture, speech, and the evolution of right-handedness. *Behav. Brain Sci.* **26**, 199–208, discussion 208–260 (2003).
29. B. Mazoyer *et al.*, Gaussian mixture modeling of hemispheric lateralization for language in a large sample of healthy individuals balanced for handedness. *PLoS One* **9**, e101165 (2014).
30. L. Van der Haegen, M. Brysbaert, The relationship between behavioral language laterality, face laterality and language performance in left-handers. *PLoS One* **13**, e0208696 (2018).
31. S. Knecht *et al.*, Handedness and hemispheric language dominance in healthy humans. *Brain* **123**, 2512–2518 (2000).
32. M. C. Corballis, The evolution of lateralized brain circuits. *Front. Psychol.* **8**, 1021 (2017).
33. D. N. Greve *et al.*, A surface-based analysis of language lateralization and cortical asymmetry. *J. Cogn. Neurosci.* **25**, 1477–1492 (2013).
34. S. Maingault, N. Tzourio-Mazoyer, B. Mazoyer, F. Crivello, Regional correlations between cortical thickness and surface area asymmetries: A surface-based morphometry study of 250 adults. *Neuropsychologia* **93**, 350–364 (2016).
35. C. G. F. de Kovel, C. Francks, The molecular genetics of hand preference revisited. *Sci. Rep.* **9**, 5986 (2019).
36. G. Cuellar-Partida *et al.*, Genome-wide association study identifies 48 common genetic variants associated with handedness. *Nat. Hum. Behav.* **5**, 59–70 (2021).
37. S. E. Medland *et al.*, Genetic influences on handedness: Data from 25,732 Australian and Dutch twin families. *Neuropsychologia* **47**, 330–337 (2009).
38. T. Yarkoni, R. A. Poldrack, T. E. Nichols, D. C. Van Essen, T. D. Wager, Large-scale automated synthesis of human functional neuroimaging data. *Nat. Methods* **8**, 665–670 (2011).
39. L. Labache *et al.*, A SENtence Supramodal Areas AtlaS (SENSAAS) based on multiple task-induced activation mapping and graph analysis of intrinsic connectivity in 144 healthy right-handers. *Brain Struct. Funct.* **224**, 859–882 (2019).
40. D. P. Carey, L. T. Johnstone, Quantifying cerebral asymmetries for language in dextrals and adextrals with random-effects meta analysis. *Front. Psychol.* **5**, 1128 (2014).
41. J. Yang, S. H. Lee, M. E. Goddard, P. M. Visscher, GCTA: A tool for genome-wide complex trait analysis. *Am. J. Hum. Genet.* **88**, 76–82 (2011).
42. T. Ge, C. Y. Chen, Y. Ni, Y. A. Feng, J. W. Smoller, Polygenic prediction via Bayesian regression and continuous shrinkage priors. *Nat. Commun.* **10**, 1776 (2019).
43. O. Reish *et al.*, A homozygous Nme7 mutation is associated with situs inversus totalis. *Hum. Mutat.* **37**, 727–731 (2016).
44. A. N. Mohebiany, S. Harroch, S. Bouyain, New insights into the roles of the contactin cell adhesion molecules in neural development. *Adv. Neurobiol.* **8**, 165–194 (2014).
45. F. Alzahrani, T. H. Albatti, F. S. Alkuraya, A de novo ATXN2L variant in a child with developmental delay and macrocephaly. *Am. J. Med. Genet. A.* **185**, 949–951 (2021).
46. C. Chiarello, D. Vazquez, A. Felton, C. M. Leonard, Structural asymmetry of anterior insula: Behavioral correlates and individual differences. *Brain Lang.* **126**, 109–122 (2013).
47. L. O'Regan, D. J. Serrien, Individual differences and hemispheric asymmetries for language and spatial attention. *Front. Hum. Neurosci.* **12**, 380 (2018).
48. D. V. M. Bishop, Cerebral asymmetry and language development: Cause, correlate, or consequence? *Science* **340**, 1230531 (2013).
49. J. Dubois *et al.*, Structural asymmetries of perisylvian regions in the preterm newborn. *Neuroimage* **52**, 32–42 (2010).
50. C. G. F. de Kovel, A. Carrión-Castillo, C. Francks, A large-scale population study of early life factors influencing left-handedness. *Sci. Rep.* **9**, 584 (2019).
51. C. McManus, Is any but a tiny fraction of handedness variance likely to be due to the external environment? *Laterality* **26**, 310–314 (2021).
52. K. J. Mitchell, *Innate: How the Wiring of Our Brains Shapes Who We Are* (Princeton University Press, Princeton, NJ, 2018).
53. Y. H. Tee *et al.*, Cellular chirality arising from the self-organization of the actin cytoskeleton. *Nat. Cell Biol.* **17**, 445–457 (2015).
54. M. Inaki, J. Liu, K. Matsuno, Cell chirality: Its origin and roles in left-right asymmetric development. *Philos. Trans. R. Soc. Lond. B Biol. Sci.* **371**, 20150403 (2016).
55. T. Okumura *et al.*, The development and evolution of left-right asymmetry in invertebrates: Lessons from *Drosophila* and snails. *Dev. Dyn.* **237**, 3497–3515 (2008).
56. A. Davison *et al.*, Formin is associated with left-right asymmetry in the pond snail and the frog. *Curr. Biol.* **26**, 654–660 (2016).
57. J. Steinhauer, D. Kalderon, Microtubule polarity and axis formation in the *Drosophila* oocyte. *Dev. Dyn.* **235**, 1455–1468 (2006).
58. M. A. McNiven, K. R. Porter, Organization of microtubules in centrosome-free cytoplasm. *J. Cell Biol.* **106**, 1593–1605 (1988).
59. M. Lobikin *et al.*, Early, nonciliary role for microtubule proteins in left-right patterning is conserved across kingdoms. *Proc. Natl. Acad. Sci. U.S.A.* **109**, 12586–12591 (2012).
60. M. C. Postema, A. Carrion-Castillo, S. E. Fisher, G. Vingerhoets, C. Francks, The genetics of situs inversus without primary ciliary dyskinesia. *Sci. Rep.* **10**, 3677 (2020).
61. I. C. McManus, N. Martin, G. F. Stubbings, E. M. Chung, H. M. Mitchison, Handedness and situs inversus in primary ciliary dyskinesia. *Proc. Biol. Sci.* **271**, 2579–2582 (2004).
62. G. Vingerhoets *et al.*, Brain structural and functional asymmetry in human situs inversus totalis. *Brain Struct. Funct.* **223**, 1937–1952 (2018).
63. S. Tanaka, R. Kanzaki, M. Yoshibayashi, T. Kamiya, M. Sugishita, Dichotic listening in patients with situs inversus: Brain asymmetry and situs asymmetry. *Neuropsychologia* **37**, 869–874 (1999).
64. D. P. Norris, Cilia, calcium and the basis of left-right asymmetry. *BMC Biol.* **10**, 102 (2012).
65. M. Fliegauf, T. Benzing, H. Omran, When cilia go bad: Cilia defects and ciliopathies. *Nat. Rev. Mol. Cell Biol.* **8**, 880–893 (2007).
66. A. Fry *et al.*, Comparison of sociodemographic and health-related characteristics of UK Biobank participants with those of the general population. *Am. J. Epidemiol.* **186**, 1026–1034 (2017).
67. A. E. Taylor *et al.*, Exploring the association of genetic factors with participation in the Avon Longitudinal Study of Parents and Children. *Int. J. Epidemiol.* **47**, 1207–1216 (2018).
68. Z. Sha, D. Schijven, C. Francks, Patterns of brain asymmetry associated with polygenic risks for autism and schizophrenia implicate language and executive functions but not brain masculinization. *Mol. Psychiatry*, 10.1038/s41380-021-01204-z (2021).
69. B. J. Ransil, S. C. Schachter, Test-retest reliability of the Edinburgh Handedness Inventory and Global Handedness preference measurements, and their correlation. *Percept. Mot. Skills* **79**, 1355–1372 (1994).
70. T. J. Crow, L. R. Crow, D. J. Done, S. Leask, Relative hand skill predicts academic ability: Global deficits at the point of hemispheric indecision. *Neuropsychologia* **36**, 1275–1282 (1998).
71. G. Badzakova-Trajkov, I. S. Häberling, M. C. Corballis, Magical ideation, creativity, handedness, and cerebral asymmetries: A combined behavioural and fMRI study. *Neuropsychologia* **49**, 2896–2903 (2011).
72. C. Bycroft *et al.*, The UK Biobank resource with deep phenotyping and genomic data. *Nature* **562**, 203–209 (2018).
73. C. Sudlow *et al.*, UK biobank: An open access resource for identifying the causes of a wide range of complex diseases of middle and old age. *PLoS Med.* **12**, e1001779 (2015).
74. K. L. Miller *et al.*, Multimodal population brain imaging in the UK Biobank prospective epidemiological study. *Nat. Neurosci.* **19**, 1523–1536 (2016).
75. F. Alfaro-Almagro *et al.*, Image processing and quality control for the first 10,000 brain imaging datasets from UK Biobank. *Neuroimage* **166**, 400–424 (2018).
76. B. Fischl, FreeSurfer. *Neuroimage* **62**, 774–781 (2012).
77. J. Yang *et al.*, Common SNPs explain a large proportion of the heritability for human height. *Nat. Genet.* **42**, 565–569 (2010).
78. S. H. Lee, J. Yang, M. E. Goddard, P. M. Visscher, N. R. Wray, Estimation of pleiotropy between complex diseases using single-nucleotide polymorphism-derived genomic relationships and restricted maximum likelihood. *Bioinformatics* **28**, 2540–2542 (2012).
79. G. Ni *et al.*, Schizophrenia Working Group of the Psychiatric Genomics Consortium; Major Depressive Disorder Working Group of the Psychiatric Genomics Consortium, A comparison of ten polygenic score methods for psychiatric disorders applied across multiple cohorts. *Biol. Psychiatry* **90**, 611–620 (2021).
80. 1000 Genomes Project Consortium, A global reference for human genetic variation. *Nature* **526**, 68–74 (2015).
81. M. J. Machiela, S. J. Chanock, LDlink: A web-based application for exploring population-specific haplotype structure and linking correlated alleles of possible functional variants. *Bioinformatics* **31**, 3555–3557 (2015).
82. Z. Sha *et al.*, Brain structural asymmetry effect maps from a study of 31,864 individuals. Max Planck Institute for Psycholinguistics Archive. https://hdl.handle.net/1839/24c1553d-3ee8-4879-8877-79ca19a0ac6a. Deposited 2 November 2021.